BIOCHEMISTRY
including biophysical chemistry & molecular biology

ARTICLE

pubs.acs.org/biochemistry

Comparative Analysis of the 15.5kD Box C/D snoRNP Core Protein in the Primitive Eukaryote *Giardia lamblia* Reveals Unique Structural and Functional Features

Shyamasri Biswas,[†] Greg Buhrman,[†] Keith Gagnon,[‡] Carla Mattos,[†] Bernard A. Brown, II,[†] and E. Stuart Maxwell[*,†]

[†]Department of Molecular and Structural Biochemistry, North Carolina State University, Raleigh, North Carolina 27695, United States

[‡]Department of Pharmacology, University of Texas Southwestern Medical Center at Dallas, Dallas, Texas 75390, United States

ABSTRACT: Box C/D ribonucleoproteins (RNP) guide the 2′-O-methylation of targeted nucleotides in archaeal and eukaryotic rRNAs. The archaeal L7Ae and eukaryotic 15.5kD box C/D RNP core protein homologues initiate RNP assembly by recognizing kink-turn (K-turn) motifs. The crystal structure of the 15.5kD core protein from the primitive eukaryote *Giardia lamblia* is described here to a resolution of 1.8 Å. The *Giardia* 15.5kD protein exhibits the typical α−β−α sandwich fold exhibited by both archaeal L7Ae and eukaryotic 15.5kD proteins. Characteristic of eukaryotic homologues, the *Giardia* 15.5kD protein binds the K-turn motif but not the variant K-loop motif. The highly conserved residues of loop 9, critical for RNA binding, also exhibit conformations similar to those of the human 15.5kD protein when bound to the K-turn motif. However, comparative sequence analysis indicated a distinct evolutionary position between Archaea and Eukarya. Indeed, assessment of the *Giardia* 15.5kD protein in denaturing experiments demonstrated an intermediate stability in protein structure when compared with that of the eukaryotic mouse 15.5kD and archaeal *Methanocaldococcus jannaschii* L7Ae proteins. Most notable was the ability of the *Giardia* 15.5kD protein to assemble in vitro a catalytically active chimeric box C/D RNP utilizing the archaeal *M. jannaschii* Nop56/58 and fibrillarin core proteins. In contrast, a catalytically competent chimeric RNP could not be assembled using the mouse 15.5kD protein. Collectively, these analyses suggest that the *G. lamblia* 15.5kD protein occupies a unique position in the evolution of this box C/D RNP core protein retaining structural and functional features characteristic of both archaeal L7Ae and higher eukaryotic 15.5kD homologues.

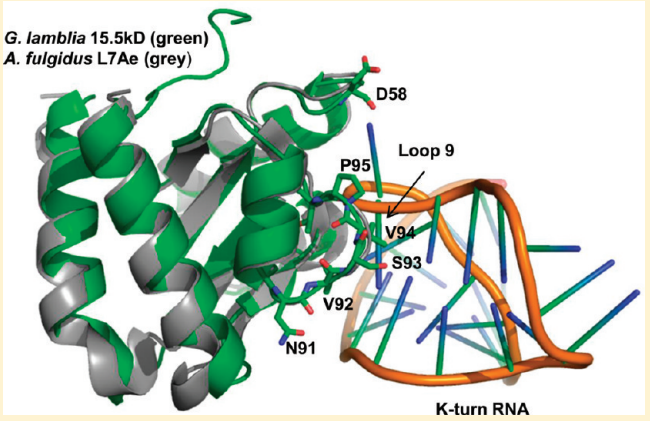

Box C/D small ribonucleoprotein complexes (snoRNPs or sRNPs) guide the 2′-O-methylation of specific nucleotides within rRNA.[1,2] These nucleotide modifications are important for both ribosome biogenesis and function. Box C/D RNAs possess conserved terminal box C and D and internal C′ and D′ nucleotide sequences that fold to establish kink-turn (K-turn) and kink-loop (K-loop) motifs, respectively.[3−5] These motifs are recognized by core proteins to assemble the box C/D and C′/D′ RNP complexes. Guide sequences located adjacent to boxes D and D′ form base pairs with complementary sequences in rRNA to determine the specific nucleotide for modification with the associated RNP core proteins catalyzing the nucleotide modification reaction.[6] Four core proteins are used to assemble the eukaryotic box C/D small nucleolar ribonucleoprotein complexes (snoRNPs). The 15.5kD core protein initiates snoRNP assembly followed by the binding of Nop56, Nop58, and the methyltransferase fibrillarin.[7−9] The highly homologous core proteins L7Ae, Nop56/58, and fibrillarin assemble the archaeal box C/D snoRNA-like ribonucleoprotein complex (sRNP).[10−13]

The eukaryotic 15.5kD and archaeal L7Ae core proteins initiate assembly of their respective box C/D RNPs by recognizing the terminal box C/D K-turn and internal C′/D′ K-loop motifs.[11,12,14,15] The K-turn motif is characterized by an asymmetric bulge flanked by short stem structures I and II.[3] Tandem-sheared G-A base pairs hydrogen bonding across the asymmetric bulge ultimately stack upon stem II, thereby stabilizing this RNA element and inducing a sharp kink or turn of 125°. For the K-loop motif, stem II is replaced by a small loop structure.[5] In vitro binding studies have demonstrated that archaeal L7Ae binds both the K-turn and K-loop motifs to initiate box C/D and C′/D′ RNP assembly, respectively.[16,17] Similar in vitro binding analysis has shown that the eukaryotic 15.5kD core protein recognizes only the box C/D K-turn.[11,16,18]

The eukaryotic and archaeal members of the L7Ae/L30 protein family share a conserved RNA binding region and

Received: December 22, 2010
Revised: February 21, 2011
Published: March 02, 2011

recognize the K-turn motif.[17] Ribosomal proteins L7Ae and rpL30e are archaeal members of this family. Family members in eukaryotes are more numerous and include 15.5kD, SBP2, Nhp2p, and Rpp38p proteins and ribosomal proteins rpL30 and rpL7a. Several of these proteins recognize multiple RNAs and thus have multiple functions as RNP proteins. Notable among these are the archaeal L7Ae and eukaryotic 15.5kD homologues. Archaeal L7Ae functions as both a ribosomal protein and a core protein of the box C/D and H/ACA sRNPs. In eukaryotes, the 15.5kD protein is a core protein of both the box C/D snoRNPs and the spliceosomal U4 small nuclear ribonucleoprotein complex (snRNP). Both L7Ae and the 15.5kD protein recognize a K-turn motif in the respective RNAs. Only archaeal L7Ae binds the variant K-loop in vitro, although recent experiments indicate that both L7Ae and 15.5kD proteins are assembled into the C′/D′ RNP complex via protein−protein interactions.[17] Numerous crystal structures of archaeal L7Ae and eukaryotic 15.5kD proteins both as free proteins and bound to the K-turn and K-loop motifs have provided detailed structural insight into binding to their respective RNAs.[19−23] Comparison of the free and RNA-bound forms of L7Ae reveals that minor changes in the overall structure result upon RNA binding, indicating an induced fit mechanism.[15,16] The structural differences required for L7Ae recognition of both the K-turn and the variant K-loop motifs versus the eukaryotic 15.5kD protein's sole recognition of the K-turn motif are just now beginning to emerge.[17]

Giardia lamblia is an intestinal parasite infecting humans that causes severe intestinal disease worldwide.[24] *G. lamblia* is classified as a primitive eukaryote, even lacking a nucleolus. The structure of the *G. lamblia* 15.5kD protein is presented here and compared with those of both its eukaryotic and archaeal homologues. Interestingly, the *Giardia* 15.5kD protein exhibits many structural features intermediate between those of archaeal *Methanocaldococcus jannaschii* L7Ae and higher eukaryotic mouse 15.5kD proteins. Similarly, biophysical analysis also suggests characteristics intermediate between those of the archaeal and higher eukaryotic homologues. Most surprisingly, the eukaryotic *Giardia* 15.5kD protein can substitute for the archaeal L7Ae protein in assembling a chimeric box C/D sRNP complex that can function in directing the 2′-O-methylation of target RNA substrates. Collectively, these results reveal that the 15.5kD box C/D RNP core protein of the primitive eukaryote *G. lamblia* exhibits unique structural features intermediate between those of the archaeal and higher eukaryotic homologues. These structural features permit its interaction with both archaeal and eukaryotic core proteins, thus facilitating both RNP assembly and box C/D RNA-guided nucleotide modification.

MATERIALS AND METHODS

Protein Expression and Purification. The 15.5kD gene was PCR-amplified from *G. lamblia* genomic DNA (ATCC) and subcloned into a pET28a vector (Novagen). This vector introduces an N-terminal His_6 tag followed by a thrombin cleavage site. Recombinant *G. lamblia* 15.5kD protein was produced in Rosetta (DE3) cells via initial growth at 37 °C until an OD_{600} of 0.6 was reached and then induction of expression via addition of 1 mM IPTG and growth at 30 °C for 3−4 h. Cells were harvested by centrifugation at 4000*g* and lysed by sonication in 10 mM HEPES (pH 7.4), 250 mM NaCl, and 10% glycerol (buffer A), and insoluble debris was removed via centrifugation at 25000*g*. Clarified lysate was applied to a nickel affinity column, and bound 15.5kD protein eluted according to the manufacturer's protocol (Qiagen). Peak fractions were pooled and concentrated. Isolated 15.5kD protein was treated with thrombin to cleave the His tag and then dialyzed against 20 mM Tris-HCl (pH 8.0), 20 mM NaCl, 0.5 mM EDTA, and 1 mM DTT. Cleaved protein was applied to a Resource-Q column (GE Healthcare) equilibrated in buffer A and eluted in a linear NaCl gradient from 20 mM to 1 M in buffer A. Concentrated protein was applied to a Superdex 200 gel filtration column (GE Healthcare) equilibrated in 20 mM HEPES (pH 7.2), 250 mM NaCl, and 5 mM DTT. Peak fractions were pooled and concentrated to 900 μM, flash-frozen in liquid nitrogen, and stored at −80 °C.

Recombinant *M. jannaschii* L7Ae and mouse 15.5kD proteins were expressed from cloned genes as previously described.[11] Mouse 15.5kD protein was prepared using the same protocol that was used to prepare the *Giardia* 15.5kD protein. The cloned *M. jannaschii* L7Ae and fibrillarin genes possess N-terminal His_6 tags. The truncated *M. jannaschii* ΔC Nop56/58 construct used in these studies consists of residues 1−367 cloned into the

Table 1. Crystallographic Data and Refinement Statistics for *G. lamblia* 15.5kD Protein

Data Reduction Statistics	
space group	*P*21
unit cell dimensions	
a, *b*, *c* (Å)	56.8, 40.6, 59.9
α, *β*, *γ* (deg)	90, 100.9, 90
resolution (Å)	50−1.8
no. of reflections	
total	361440
unique	23578 (2105)[a]
completeness (%)	95.5 (86.7)[a]
redundancy	3.1
R_{merge}[b] (%)	14.9 (33.9)[a]
Refinement Statistics	
R_{work} (%)	23.57
R_{free} (%)	25.50
root-mean-square deviation from ideal geometry	
bond lengths (Å)	0.005
bond angles (deg)	0.789
total no. of reflections	23542
Ramachandran plot analysis (%)	
most favored regions	99.59
additional allowed regions	0.41
generously allowed regions	0
disallowed regions	0
B factor (Å^2)	
average	23.694
protein backbone	21.22
protein side chains	30.34
solvent molecules	31.675
total no. of atoms	3877
no. of protein atoms	3647
no. of water molecules	221

[a] Highest-resolution bin. [b] $R_{merge} = \Sigma_{hkl}\Sigma_i|I_i(hkl) - I(hkl)|/\Sigma_{hkl}\Sigma_i|I_i(hkl)|$, where $I(hkl)$ is the observed intensity of the *i*th measurement of reflection *hkl* and $\langle I(hkl)\rangle$ is the mean intensity of reflection *hkl*.

pET21a vector between the NdeI and BamHI restriction sites and lacks the 50 C-terminal residues.[25] Fibrillarin and ΔC Nop56/58 were cotransformed into Rosetta DE3 cells, initially grown at 37 °C as described above, and protein expression was induced by addition of IPTG and continued growth overnight at 15 °C. Cells were harvested by centrifugation at 4000*g*, resuspended in buffer A, and sonicated. The sonicate was heated at 60 °C for 10 min, and after centrifugation at 25000*g*, protein was purified by nickel affinity chromatography. The ΔC Nop56/58−fibrillarin complex was further purified on a HiPrep 16/10 SP FF (GE Healthcare) column and eluted using a linear salt gradient. The purified complex was concentrated using Millipore concentrators, dialyzed against 10 mM HEPES (pH 7.2), 100 mM NaCl, 1 mM DTT, and 10% glycerol, flash-frozen, and stored at −80 °C.

Crystallization, Data Collection, and Data Processing. Purified *Giardia* 15.5kD protein was initially screened for crystallization conditions by the hanging drop vapor diffusion method using a Qiagen Classics screen (Qiagen). Initial attempts to crystallize 15.5kD protein at room temperature were unsuccessful, and crystals were obtained only at 4 °C. Diffraction quality crystals were obtained in 0.2 M ammonium sulfate, 0.1 M sodium acetate (pH 4.6), and 25% PEG 4000. A single crystal was flash-frozen in liquid nitrogen. The data set was collected at SER-CAT beamline 22ID (Advanced Photon Light Source, Argonne, IL). Data were indexed and scaled using HKL2000.[26] Data reduction statistics and unit cell parameters are listed in Table 1.

Protein Structure Determination and Refinement. The structure of *Giardia* 15.5kD protein was determined by molecular replacement using yeast Snu13p as a model.[27] The initial map and model were first obtained using PHASER (CCP4)[28] and manually fitted using COOT[29] followed by further refinement. Refinement was conducted in CNS[30] with 5% of the data excluded for the R_{free} calculation. Initially, simulated annealing with slow cooling was performed followed by energy minimization and *B* factor refinement, which substantially improved the model (R_{work} = 33.67%, and R_{free} = 35.77%). Cross-validated, sigma-A-weighted composite omit maps or sigma-A-weighted $2F_o - F_c$ and $F_o - F_c$ maps were calculated in CNS and used for fitting and model building. Density modification, implemented in CNS, was also used to reduce model bias and improve map quality. Approximately 30 iterations were performed resulting in a model with an R_{work} of 26.16% and an R_{free} of 26.57%. TLS refinement in addition to individual ADP refinement was performed using PHENIX,[31] which decreased the R_{work} and R_{free} values to 23.57 and 25.50%, respectively. Chains A and B were the two TLS groups during refinement. The final model was analyzed using PROCHECK[32] and MOLPROBITY.[33] Root-mean-square deviation (rmsd) calculations were conducted using LSQMAN.[34] All figures were constructed using PYMOL.[35]

Phylogenetic Analysis. Primary sequence alignments of archaeal L7Ae and eukaryotic 15.5kD proteins were performed using ClustalW,[36] with the resultant alignments being imported into MEGA4.[37] The bootstrap consensus tree was constructed using the neighbor joining method.

Circular Dichroism. Thermal denaturation experiments were conducted from 4 to 89 °C, monitoring ellipticity in 1 nm steps during wavelength scans from 190 to 250 nm. The difference spectrum at the two temperatures was analyzed, and denaturation was monitored at a constant wavelength of 222 nm. A protein concentration of 20 μM in 20 mM cacodylate (pH 7.2), 1 mM $MgCl_2$, 50 mM NaCl, and 50 mM KCl buffer was used for both thermal and urea denaturation studies. A temperature ramp of 1 °C/min was applied with equilibration for 0.5 min at each temperature, and ellipticity data were collected for 20 s intervals. The melting temperature and van't Hoff enthalpy of denaturation were determined from a plot of ellipticity at 222 nm versus temperature (kelvin). The melting curve was fit to a six-variable equation (assuming a two-state transition) implemented in ORIGIN 7.0 (Microcal).[38] Urea denaturation studies were conducted via titration of each protein in the same buffer as described above at different denaturant urea concentrations ranging from 0 to 5 M for *G. lamblia* and mouse 15.5kD proteins and from 0 to 11 M for *M. jannaschii* L7Ae. Protein samples were equilibrated at the respective denaturant concentrations for 30 min. Ellipticity at 22 °C was monitored at 224 nm with 10 repeats for each sample. Respective buffer control samples were subtracted to obtain final values. Plots of the average ellipticity at 224 nm versus urea concentration were constructed, and the free energy of denaturation (ΔG_D) was obtained by fitting the curves with a two-state denaturation model using ORIGIN 7.0.

In Vitro RNA Synthesis, Electrophoretic Mobility Shift Analysis, and in Vitro Methylation of Target RNAs. sR8 and U15 RNAs were synthesized by in vitro transcription and purified as previously described.[11] C/D and C′/D′ half-mers were purified by denaturing gel electrophoresis. Assembly of RNP complexes was analyzed by electrophoretic mobility shift analysis (EMSA) as previously described.[11,16] Briefly, RNA was radiolabeled with ^{32}P at the 5′ end and purified before incubation with the various box C/D RNP core proteins at 30 °C for 30 min. Assembled complexes were resolved on native, phosphate-buffered 6% polyacrylamide gels and visualized using a Molecular Dynamics PhosphoImager or by autoradiography. Assessment of RNA-guided 2′-O-methylation was conducted as previously described.[11,16] Briefly, assembled sRNP complexes were incubated at 60 °C and small aliquots removed at different time intervals. After precipitation of TCA onto filters followed by washing, incorporation of $[^3H]CH_3$ into the D and D′ target RNAs was assessed by scintillation counting.

RESULTS

***G. lamblia* 15.5kD Protein Crystal Structure.** The box C/D snoRNP 15.5kD core protein from the primitive eukaryote *G. lamblia* was isolated and the crystal structure determined for structural analysis. The crystal structure of *Giardia* 15.5kD protein was determined by molecular replacement using yeast Snu13p as the model protein.[27] Crystals have the symmetry of space group *P*21 with two molecules in the asymmetric unit (chains A and B in Figure 1A). The unit cell parameters and data reduction statistics are listed in Table 1. These two molecules were packed making a 45° angle with each other, with α1 and α4 forming the interface between the two A and B chains. Helix α1 of chain A is oriented opposite to helix α4 of chain B and vice versa. The three-dimensional structure of *Giardia* 15.5kD protein possesses a typical α−β−α sandwich fold with alternating α-helices and β-strands (Figure 1B). These strands and helices are separated by coiled regions or loops. The β-sheet core region is sandwiched between the α-helices. The three α1, α4, and α5 helices are oriented perpendicular to the α2, α3, and 3_{10} helices. The β-sheets consist of three parallel β-strands (β1−β3) and one antiparallel strand (β4). The central β-sheet core region, with the exception of β1, is composed of hydrophobic amino acid residues, whereas the α-helices are amphipathic, with the hydrophobic residues pointing inward toward the protein core and

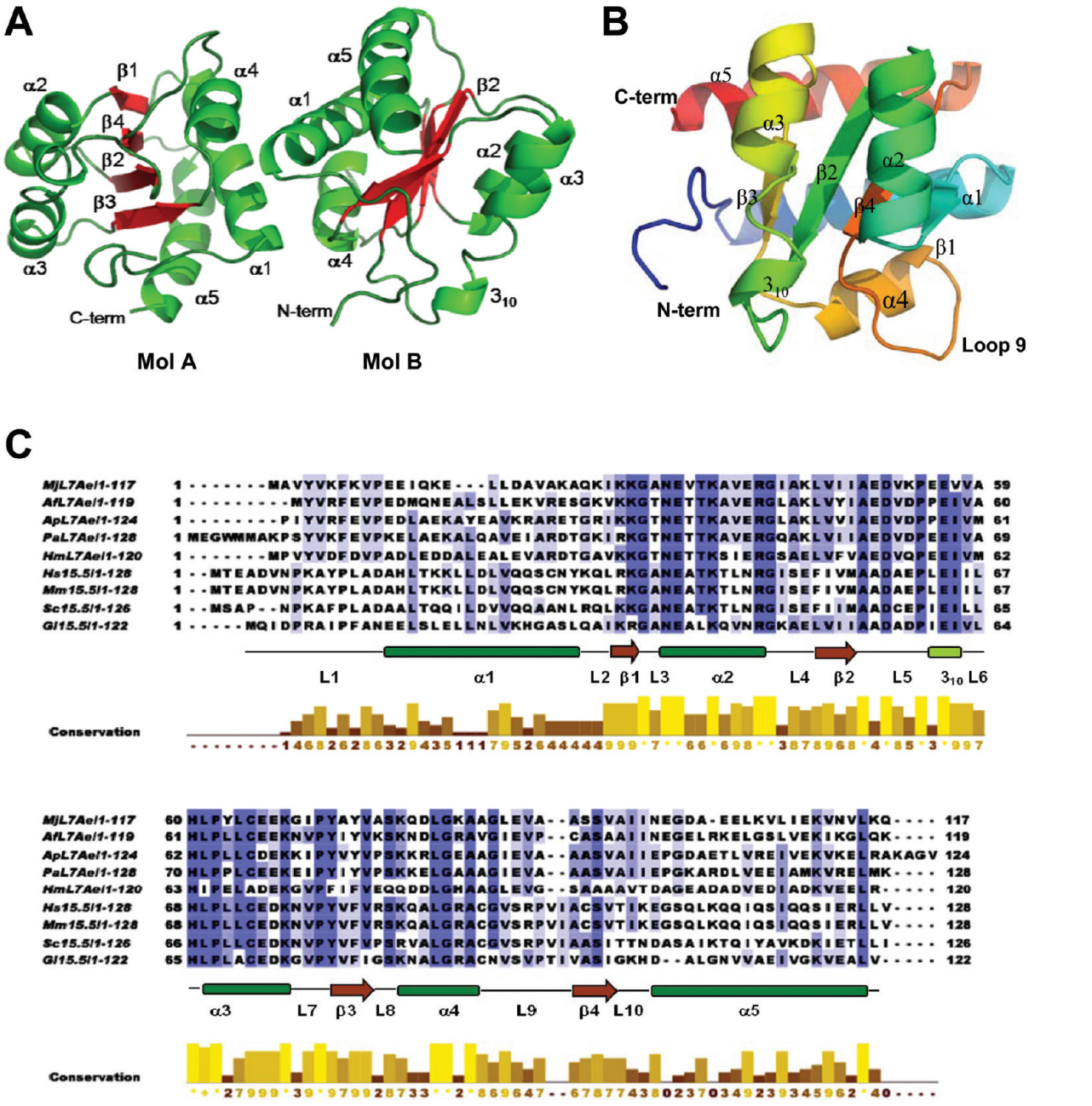

Figure 1. Structure of *G. lamblia* 15.5kD core protein. (A) Ribbon representation of the arrangement of the two molecules (MolA and MolB) in the asymmetric unit of the crystal. The α-helices (green) and *β*-strands (red) are shown. (B) Ribbon representation of the *G. lamblia* 15.5kD protein structure determined by X-ray crystallography. The α-helices and *β*-strands are indicated along with loop 9 critical for K-turn binding. (C) Sequence alignment of archaeal L7Ae and eukaryotic 15.5kD protein primary sequences. Alignment of five archaeal L7Ae [*M. jannaschii* (Mj), *Archaeoglobus fulgidus* (Af), *Aeropyrum pernix* (Ap), *Haloarcula marismortui* (Hm), and *Pyrococcus abyssi* (Pa)] and three eukaryotic 15.5kD [*Homo sapiens* (Hs), *Mus musculus* (Ms), and *Saccharomyces cerevisiae* (Sc)] homologues shaded with respect to sequence conservation. Also shown is the secondary structure of *Giardia* 15.5kD protein with the positions of the α-helices (green), *β*-strands (red), and loop regions (black lines). The conservation of each residue is presented on a scale from 0 to 10, where 0 and 10 correspond to 0 and 100% conservation, respectively.

hydrophilic residues directed outward. The 10-residue N-terminus forms an extensive hydrogen bonding network with nearby water molecules. In addition, residue D4 makes a salt bridge with R6, providing additional stability to this region and thus presenting an ordered N-terminal region in the crystal structure. The presented structure has most of the residues modeled except the D105 residue in both chains that has been modeled as a glycine and the E91 residue in chain A that is modeled as alanine because of weak densities. The N-terminus of chain A starts from I3 and chain B from G2 and I3. The loop 10−α5 region is disordered and is marked by high *B* factor values. The final model possesses 221 water molecules associated with the 119 residues of chain A and the 120 residues of chain B. The structure was refined using CNS[31] and PHENIX[32] to a final resolution of 1.85 Å. The stereochemistry and statistics of the model are listed in Table 1.

dx.doi.org/10.1021/bi1020474 |*Biochemistry* 2011, 50, 2907–2918

Table 2. Cα Root-Mean-Square Deviations Calculated with Chain B of the *Giardia* 15.5kD Structure

organism	protein name	PDB entry	Cα rmsd (Å)
Pyrococcus abyssii	L7Ae	1PXW	1.197 (117 atoms)
Aeropyrum pernix	L7Ae	2FC3	1.042 (107 atoms)
Archaeoglobus fulgidus	L7Ae	1RLG	1.14 (109 atoms)
Methanocaldococcus jannaschii	L7Ae	1RA4	0.932 (108 atoms)
Pyrococcus furiosus	L7Ae	2HVY	1.061 (112 atoms)
Sulfolobus solfataricus	L7Ae	3ID5	1.130 (113 atoms)
Saccharomyces cerevisiae	Snu13p	1ZWZ	0.833 (120 atoms)
Homo sapiens	15.5kD	1E7K	0.767 (121 atoms)

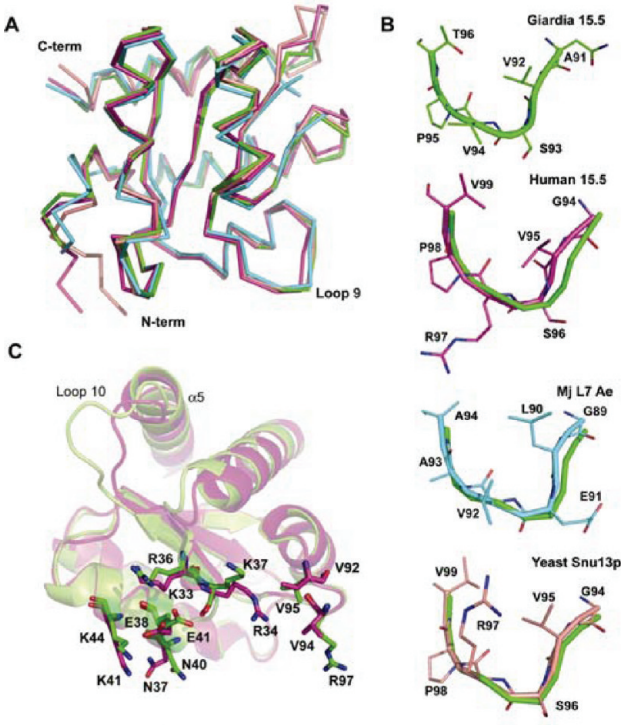

Figure 2. Comparative overlay of 15.5kD and L7Ae homologues with *G. lamblia* L7Ae. (A) Ribbon representation of superimposed Cα backbones of yeast Snu13p (salmon), human 15.5kD (pink), *M. jannaschii* L7Ae (cyan), and *Giardia* 15.5kD (green) homologues. RNA-binding loop 9 along with the N- and C-termini is indicated. (B) Side chains of the highly conserved loop 9 residues. The loop 9 Cα backbone of *Giardia* 15.5kD protein (green, top) is superimposed with human 15.5kD (pink), *M. jannaschii* L7 (cyan), and yeast Snu13p (salmon) proteins. (C) Superimposition of RNA-bound human 15.5kD protein (pink) with *Giardia* 15.5kD protein (green). Key residues involved in K-turn recognition of the human protein are colored pink and the corresponding *Giardia* residues green. Differences in the loop 10−α5 region are shown.

Comparison of the Structure of *Giardia* 15.5kD Protein with Those of Eukaryotic and Archaeal Homologues. The crystal structure of the *G. lamblia* 15.5kD core protein is very similar to those of yeast Snu13p, human 15.5kD, and archaeal L7Ae homologues. Calculated Cα rmsd values revealed that the *Giardia* 15.5kD protein is more similar to the eukaryotic human and yeast homologues than to the archaeal L7Ae proteins (Table 2), which is expected. However, further inspection did

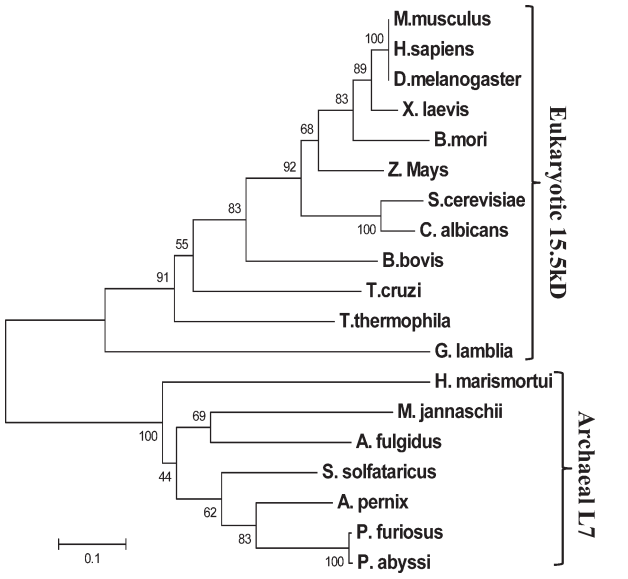

Figure 3. Phylogenetic tree of eukaryotic 15.5kD and archaeal L7Ae protein evolution.

reveal distinct differences between the *Giardia* protein and the eukaryotic and archaeal homologues. The N-terminus of *Giardia* 15.5kD protein is shorter than that of either the human 15.5kD or yeast Snu13p protein, more closely resembling that of the archaeal L7Ae proteins (Figures 1C and 2A). Sequence alignment revealed that the *Giardia* 15.5kD amino acid side chains of the β1−loop 3−α2, loop 5−3_{10} helix, and loop 9 regions implicated in K-turn binding are well-conserved and most closely aligned with those of the eukaryotic homologues (Figure 1C). These include the loop 9 residues (VSRP) that are critical for eukaryotic 15.5kD protein K-turn binding as well as its lack of K-loop recognition.[17,20] The *Giardia* 15.5kD amino acids (VSVP) (Figure 2B) sharply contrast with the corresponding archaeal loop 9 residues (LEVA). Analysis of human 15.5kD protein bound to K-turn RNA has indicated that residues K37, N40, E41, K44, V95, and R97 interact with the RNA. The closely corresponding residues in *Giardia* 15.5kD protein are R34, N37, E38, K41, V92, and V95 (Figure 2C).

A major difference noted between the *Giardia* 15.5kD structure and the human and yeast structure lies in the loop 10−α5 region. For *Giardia* 15.5kD protein, loop 10 is shorter by two residues and α5 is one turn longer. The electron density of this region is weak in the *Giardia* structure and is marked with high *B* factor values indicating greater flexibility. However, high flexibility has been observed in all known eukaryotic 15.5kD and archaeal L7Ae protein structures, suggesting that this region of the protein may ultimately be involved in core protein binding and/or RNA interaction during sRNP assembly. Notable is the intermediate length of loop 10 in the *Giardia* 15.5kD protein structure when compared with those of *M. jannaschii* L7Ae and the yeast and human 15.5kD homologues. *M. jannaschii* L7Ae[15] has a Cα rmsd of 0.93 Å (108 atoms) compared with *Giardia* 15.5kD protein. An overlay of the two structures revealed differences in loop 2, α1, and the loop 10−β4 region. Loop 2 is shorter and β1 longer for the archaeal L7Ae proteins. The archaeal proteins also possess a longer β4 with a shorter loop 10 when compared with those of *Giardia* 15.5kD protein (Figure 2A). Calculated Cα rmsd values of determined archaeal

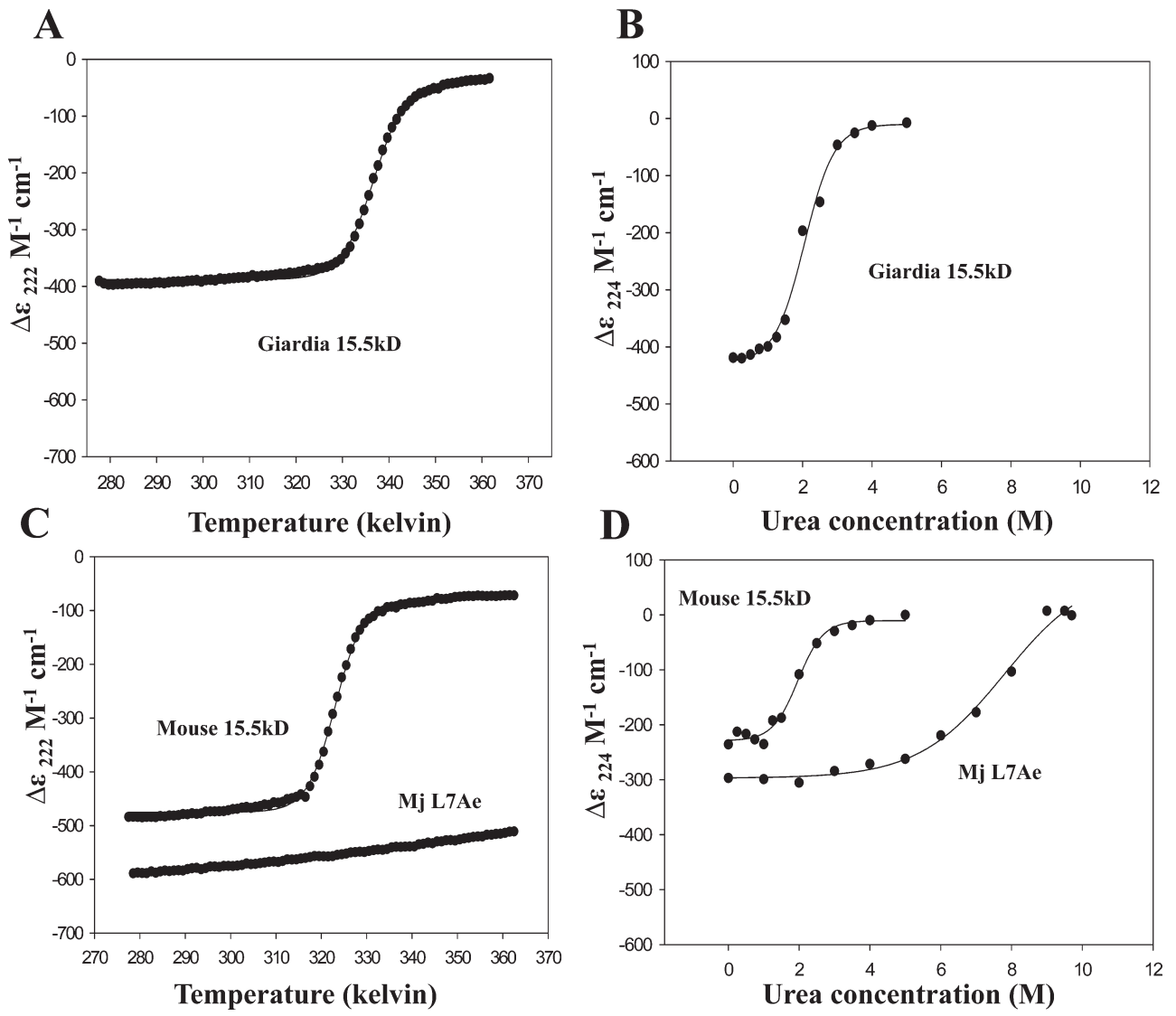

Figure 4. Stability of *G. lamblia* 15.5kD protein structure. (A) Thermal denaturation of *Giardia* 15.5kD protein monitored by circular dichroism spectroscopy. Protein denaturation was monitored at 222 nm to determine the melting temperature of 63 °C. (B) Chemical denaturation of *Giardia* 15.5kD protein. The 15.5kD protein was treated with increasing concentrations of urea and protein denaturation monitored using circular dichroism spectroscopy at 224 nm. (C) Comparative melting curves of mouse 15.5kD and *M. jannaschii* L7Ae proteins monitored by circular dichroism spectroscopy at 222 nm. (D) Comparative denaturation of mouse 15.5kD and *M. jannaschii* wild-type L7Ae proteins treated with increasing urea concentrations and monitored using circular dichroism spectroscopy at 224 nm.

L7Ae structures varied from 0.9 to 1.2 Å (Table 2) with the maximal difference in Cα atoms observed in the *P. abyssi* L7Ae[23] structure, mainly due to an unusually long N-terminal region.

Finally, the sequence relationship of *Giardia* 15.5kD protein with its archaeal and eukaryotic homologues was examined by alignment of L7Ae and 15.5kD proteins with the subsequent construction of a phylogenetic tree (Figure 3). *Giardia* 15.5kD protein is clearly grouped with the eukaryotic 15.5kD homologues. However, *Giardia* 15.5kD protein diverges early in evolution from the eukaryotic 15.5kD proteins soon after divergence of Archaea and Eukarya. This is consistent with our structural observations indicating an intermediate position for *Giardia* 15.5kD protein between L7Ae and the higher eukaryotic 15.5kD proteins.

Stability of the *G. lamblia* 15.5kD Core Protein. To further compare the structural features of *Giardia* 15.5kD protein with those of archaeal L7Ae and higher eukaryotic 15.5kDa proteins, physical studies were undertaken. The stability of the *Giardia* 15.5kD core protein was investigated by thermal and chemical denaturation studies using circular dichroism spectroscopy. Although *Giardia* typically grows at 37 °C, it can survive under harsh environmental conditions by forming cysts.[24] Protein thermal melts were used to monitor the change in protein secondary structure with an increase in temperature. A melting temperature of 63 °C (336 ± 0.55 K) was determined, and the van't Hoff denaturation enthalpy was calculated to be 78.8 ± 0.95 kcal/mol from a best fit analysis of the data (Figure 4A). In comparison, the mouse 15.5kD protein revealed a lower melting temperature (52 °C), whereas archaeal L7Ae exhibited a considerably higher T_m (Figure 4C). Indeed, previous studies from our laboratories demonstrated for *M. jannaschii* L7Ae a melting temperature exceeding 90 °C and estimated at 107 ± 5 °C (380.5 K).[15] The stabilities of these proteins were also assessed by

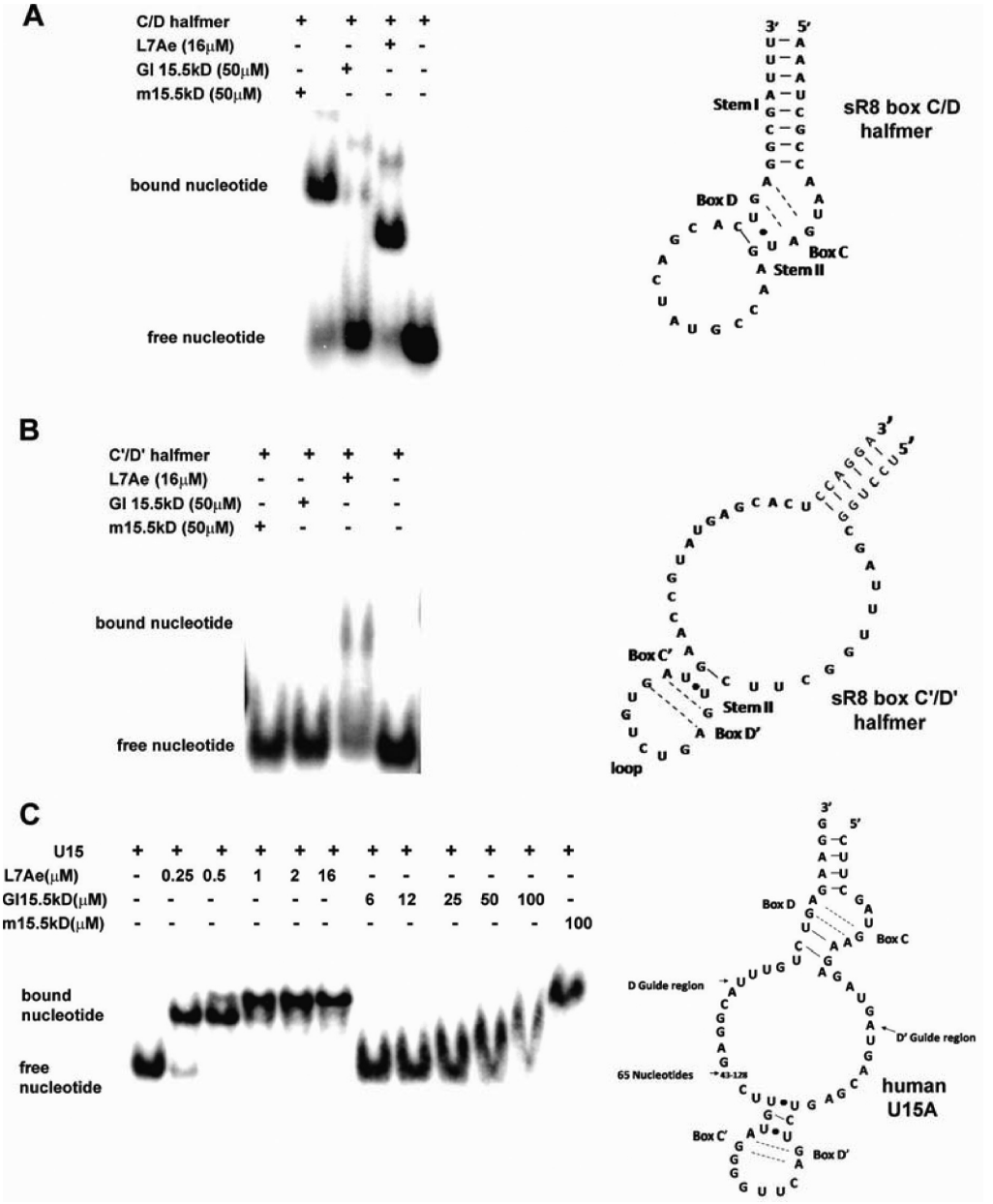

Figure 5. *Giardia* 15.5kD protein binds the K-turn but not the K-loop motif. Binding of *Giardia* 15.5kD protein to the K-turn and K-loop motifs was assessed via electrophoretic mobility shift analysis (EMSA). Radiolabeled RNA possessing the box C/D (K-turn) and/or C′/D′ (K-loop) motifs was incubated with *Giardia* 15.5kD, mouse 15.5kD, or *M. jannaschii* L7Ae protein, and the assembled RNA−protein complexes were resolved on native polyacrylamide gels and revealed by autoradiography. The various incubated RNAs and proteins used in individual EMSA reactions are indicated above the respective gel lanes. The structure and sequence of the respective RNAs are indicated at the right with C/D (K-turn) and C′/D′ (K-loop) boxes designated: (A) 15.5kD and L7Ae proteins binding to the sR8 half-mer possessing the box C/D motif (K-turn), (B) 15.5kD and L7Ae proteins binding to the sR8 half-mer possessing the C′/D′ motif (K-loop), and (C) 15.5kD and L7Ae proteins binding to human U15A box C/D snoRNA possessing both box C/D and C′/D′ motifs. Concentrations of the titrated proteins are indicated above the respective gel lanes.

chemical denaturation studies using the chaotropic agent urea. The denaturation midpoint for *Giardia* 15.5kD protein was 2.5 M (Figure 4B) in comparison with 2.3 M (Figure 4D) and 6.9 M for the mouse and archaeal homologues, respectively. The high number of short-range ionic interactions is assumed to account for the high thermal stability of the archaeal L7Ae protein. For the *Giardia* 15.5kD protein, a ΔG_D value of 2.46 ± 0.89 kcal mol^{-1} and an *m* value of −1.30 ± 0.39 kcal mol^{-1} M^{-1} were calculated from the denaturation curve. These values are also lower in comparison to those for urea denaturation of the archaeal *M. jannaschii* L7Ae protein (ΔG_D of 8.72.5 kcal mol^{-1} and *m* value of 1.3 ± 0.39 kcal mol^{-1} M^{-1}). For each of the biophysical analyses, the *Giardia* 15.5kD protein occupied an intermediate position between the eukaryotic mouse and the archaeal homologues.

The *Giardia* 15.5kD Protein Exhibits RNA Binding Capabilities Characteristic of Its Eukaryotic Homologues. Binding of *Giardia* and mouse 15.5kD and *M. jannaschii* L7Ae proteins to the K-turn and K-loop motifs was assessed via EMSA. Previous work has demonstrated that the archaeal L7Ae core

dx.doi.org/10.1021/bi1020474 |*Biochemistry* 2011, 50, 2907–2918

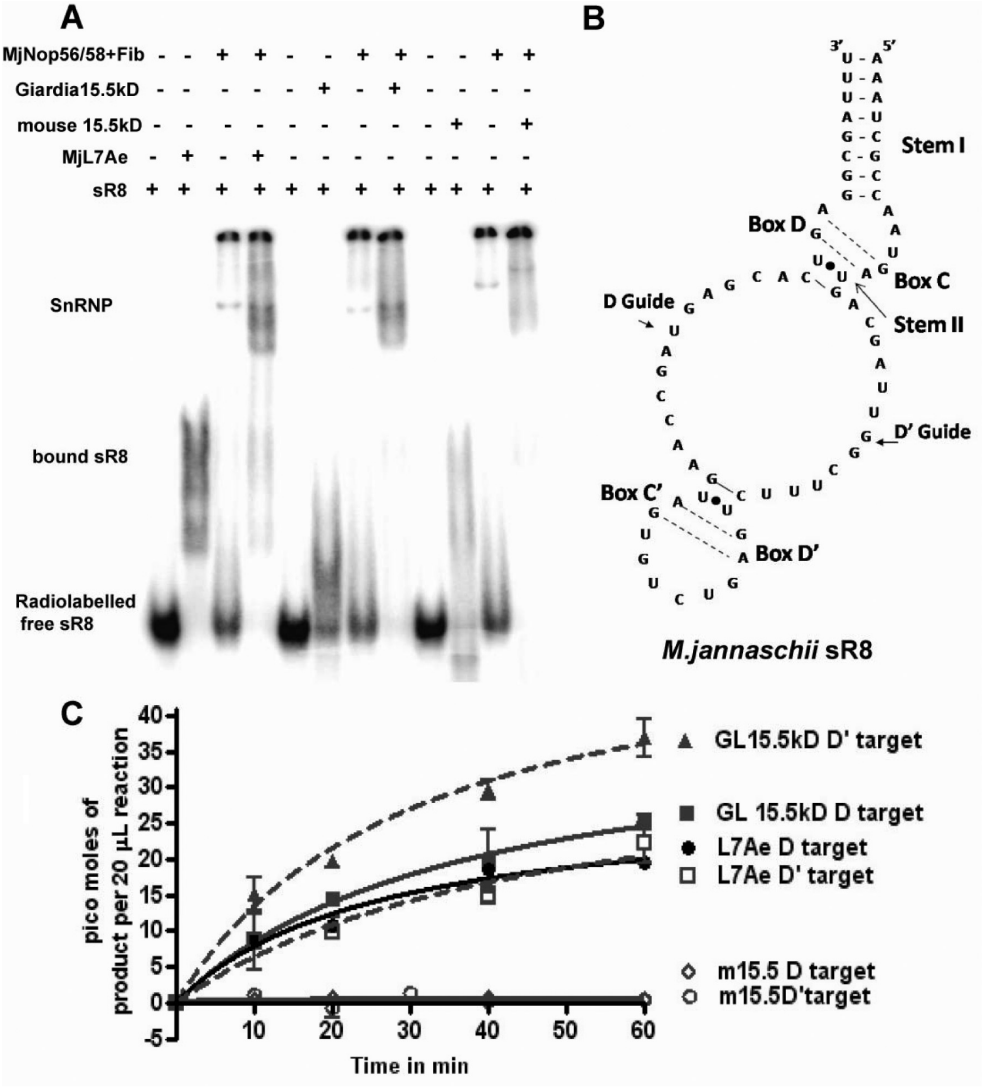

Figure 6. In vitro-assembled chimeric *Giardia*−archaeal box C/D RNPs possess methyltransferase activity. (A) Electrophoretic mobility shift analysis of chimeric box C/D RNPs assembled with eukaryotic and archaeal core proteins. Radiolabeled sR8 sRNA possessing box C/D and C′/D′ motifs was incubated with combinations of *M. jannaschii*, mouse, and *Giardia* core proteins, and the assembled RNPs were resolved on native polyacrylamide gels and revealed by autoradiography. The various combinations of sR8 with box C/D RNP core proteins are indicated above the respective gel lanes. (B) Sequence and folded structure of *M. jannaschii* sR8 box C/D sRNA possessing the terminal box C/D and internal C′/D′ motifs. Boxes C, C′, D, and D′ are indicated along with the D and D′ guide sequences used to direct sRNA-guided nucleotide modification. (C) In vitro methyltransferase activity of the assembled chimeric box C/D RNPs. Assembled RNPs were incubated with [^{3}H]-*S*-adenosylmethionine, and methyltransferase activity was determined by incorporation of [^{3}H]CH_3 into D and D′ target RNAs.

protein binds both the K-turn (box C/D) and K-loop (C′/D′) motifs in vitro whereas eukaryotic 15.5kD protein recognizes only the K-turn motif.[11,16,18] Therefore, all three core protein homologues were examined for binding to the *M. jannaschii* sR8 box C/D and C′/D′ half-mer RNAs. *M. jannashii* L7Ae and mouse 15.5kD protein bound the box C/D K-turn motif strongly, with the *Giardia* 15.5kD protein binding less strongly (Figure 5A). Notably and as expected, the archaeal L7Ae protein was the only homologue able to recognize and stably bind the sR8 C′/D′ RNA half-mer (K-loop motif) (Figure 5B). The strength of binding of the *Giardia* 15.5kD protein to human U15A snoRNA was further assessed in titration experiments (Figure 5C). *M. jannaschii* L7Ae bound to both U15A K-turn and K-loop motifs as evidenced by the sequential formation of two RNP complexes. Titration of *Giardia* 15.5kD protein over similar protein concentrations again demonstrated a reduced binding affinity with the gradual formation of an RNP complex of increasing size with increasing protein concentrations. This binding curve is symptomatic of a more weakly binding protein recognizing an RNA motif under the nonequilibrium binding conditions experienced with EMSA. Comparison of the *Giardia* and mouse 15.5kD proteins at equal concentrations of 100 μM revealed the stronger recognition of the mouse versus the *Giardia* protein. Thus, the binding characteristics of the *Giardia* 15.5kD core protein were most typical, albeit at a reduced strength, with respect to eukaryotic 15.5kD homologues.

RNP Assembly and Methyltransferase Activity of a Chimeric Eukaryotic−Archaeal Box C/D RNP. Both structural analysis and biophysical examinations suggested that the *Giardia* 15.5kD core protein occupies an intermediate position between

the higher eukaryotic and archaeal homologues. Therefore, the catalytic or functional activity of this primordial eukaryote's core protein was subsequently assessed using the archaeal sRNP in vitro assembly system, which reconstitutes a methyltransferase-competent ribonucleoprotein complex using recombinant core proteins and in vitro transcribed box C/D sRNA.[11,12] Using this assembly system, recombinant *Giardia*, mouse, or *M. jannaschii* 15.5kD and L7Ae core proteins were assembled with archaeal sR8 box C/D sRNA and the *M. jannaschii* Nop56/58 and fibrillarin core proteins.

EMSA again revealed that *Giardia* 15.5kD protein binds archaeal sR8 sRNA weakly (Figure 6A), recognizing the well-conserved K-turn of the terminal box C/D motif but not the K-loop (Figure 6B). Unexpectedly, however, the archaeal Nop56/58−fibrillarin complex was able also to bind the *Giardia* L7Ae−sR8 sRNA complex assembling a complete sRNP, with a migration similar to that of the sRNP assembled with all *M. jannaschii* core proteins. In contrast, a larger sRNP was not formed when the archaeal Nop56/58−fibrillarin complex was incubated with the mouse 15.5kD protein−sR8 sRNA complex. (The strong bands in those lanes where the RNP mixture includes Nop56/58 and fibrillarin result from aggregation in the sample wells of the gel.) A faint higher-molecular mass band was observed in the gel shift assay (Figure 6A, far right lane). We suspect this is likely the Nop56/58−fibrillarin dimer binding sR8 nonspecifically without associated mouse 15.5kD protein. These observations indicated that the *Giardia* 15.5kD protein has retained sufficient structural homology with the archaeal L7Ae protein to retain its ability to interact with the Nop56/58−fibrillarin complex and assemble a complete sRNP complex possessing three core proteins on both the terminal box C/D and internal C′/D′ motifs.

Subsequent analysis examined the methyltransferase activity of the sR8 sRNPs assembled with either the archaeal L7Ae or *Giardia* 15.5kD core protein homologues. Surprisingly, the sRNP assembly using the *Giardia* core protein efficiently guided nucleotide modification from both the box C/D and C′/D′ RNPs (Figure 6C). As expected because of incomplete sRNP assembly, attempts to methylate the D and D′ target RNAs with an sRNP complex using the mouse 15.5kD core protein revealed no methyltransferase activity guided by either the box C/D or C′/D′ RNPs. Thus, not only was the eukaryotic *Giardia* 15.5kD protein allowing "archaeal" box C/D sRNP assembly, it also facilitated the methyltransferase activity of this chimeric complex.

DISCUSSION

The 15.5kD and L7Ae proteins play critical roles in box C/D RNP structure and function by binding the K-turn motifs to initiate assembly of the eukaryotic and archaeal box C/D RNP nucleotide modification complexes. The crystal structure of the 15.5kD protein from the primitive eukaryote *G. lamblia* has now been determined to 1.8 Å resolution revealing an α−β−α sandwich fold structure. Comparative structural and phylogenetic analysis has suggested an intermediate structural position with respect to its higher eukaryotic and archaeal homologues. Biophysical examination determining the denaturation properties of the folded structure of *Giardia* 15.5kD protein was consistent with such an intermediary structure. As expected for a eukaryotic homologue, *Giardia* 15.5kD protein binds the K-turn but not the K-loop motif of the box C/D RNAs. Unexpectedly, however, it can assemble a chimeric box C/D RNP with archaeal core proteins that is catalytically active and 2′-O-methylates target RNAs. Thus, *Giardia* 15.5kD protein possesses structural features that allow protein−protein interactions with both the archaeal and eukaryotic box C/D RNP core proteins to facilitate methyltransferase activity.

Examination of the crystal structure of *Giardia* 15.5kD protein revealed an α−β−α sandwich fold, typical of several eukaryotic 15.5kD and archaeal L7Ae homologues previously examined by crystallographic analysis. The 15.5kD and L7Ae homologues are members of the L7/L30 protein family whose shared characteristic is the ability to bind the K-turn motif. The archaeal L7Ae homologues are unique in that they are also able to recognize the K-loop motif. In addition to the 15.5kD and L7Ae proteins, this family includes archaeal rpL30e and eukaryotic rpL30, rpL7a, Nhp2p, SBP2, and Rpp38p proteins. For these proteins, only the crystal structure of eukaryotic rpL30 has been determined, and it also exhibits an expected α−β−α sandwich fold.[39] Modeling and structure predictions of the other family members have indeed indicated that they also share this same structural motif in their respective RNA binding domains.[40−42] Comparative analysis revealed that the *Giardia* 15.5kD protein's Cα backbone rmsd is closer to those of the yeast and mouse eukaryotic homologues (Table 2). However, the shorter loop regions and long N-terminal regions are characteristic of the archaeal homologues. Thus, *Giardia* 15.5kD protein exhibits structural features found in both higher eukaryotic and archaeal homologues.

The *Giardia* 15.5kD protein shares with the higher eukaryotic homologues those amino acids important for RNA binding. These human 15.5kD protein residues K37, N40, E41, K44, V95, and R97 are *Giardia* 15.5kD protein amino acids R34, N37, E38, K41, V92, and V95, respectively.[4] Of particular importance are the loop 9 amino acids that directly interact with the K-turn motif. Notably, these highly conserved amino acids are distinct for the eukaryotic and archaeal domains.[17] The eukaryotic loop 9 signature amino acids (VSRP) are replaced by a LEVA motif in the archaeal proteins. The *Giardia* 15.5kD protein loop 9 amino acids are characteristic of the eukaryotic homologues with a VSVP motif, although the third amino acid (V) is that seen in L7Ae proteins. It is these archaeal amino acids (LEVA) that allow L7Ae to bind the K-loop motif comprised of internal C′/D′ boxes. Notably, replacement of archaeal amino acids LEVA with eukaryotic residues VSRP results in the inability of L7Ae to recognize the K-loop.[17] Individual mutagenesis of all four signature amino acids has also shown that the two internal are most important for K-turn and K-loop recognition. For *Giardia* 15.5kD protein, one of these internal residues is archaeal in character (V for R). Previous mutagenesis has indeed revealed that mutating the eukaryotic loop 9 signature amino acids (VSRP) to a VSVP motif significantly weakens binding to the K-turn.[17] Thus, the observed weak binding of *Giardia* 15.5kD protein to the K-turn is a consequence of its loop 9 signature amino acid sequence (VSVP).

Superimposition of the *Giardia* 15.5kD protein over that of *Ar. fulgidus* L7Ae bound to a K-turn RNA shows that the 15.5kD protein loop 9 serine and valine residues are considerably shorter in comparison with the glutamate residue of L7Ae (Figure 7). In addition, the long loop 9 arginine side chain of human 15.5kD protein that makes significant interaction with the RNA molecule[4] is absent in *Giardia* 15.5kD protein. The presence of an uncharged amino acid at this position could also be expected to contribute to the low binding affinity as the arginine of human 15.5kD protein forms a salt bridge with the phosphate backbone

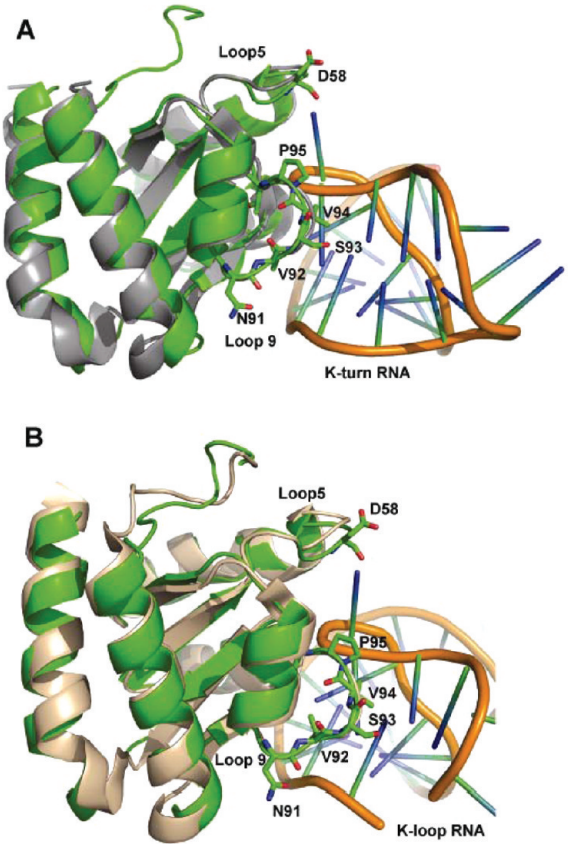

Figure 7. Superimposed structures of *G. lamblia* 15.5kD protein with *Ar. fulgidus and P. furiosus* L7Ae bound to K-turn and K-loop motifs, respectively. *Giardia* 15.5kD protein (green) is superimposed on *Ar. fulgidus* (PDB entry 1RLG) L7Ae (gray) bound to a box C/D K-turn (A) and *P. furiosus* (wheat) L7Ae (PDB entry 2HVY) bound to a C′/D′ K-loop (B). Loop 9 (N91, V92, S93, V94, and P95) and loop 5 (D58) residues critical for RNA binding are shown on *Giardia* 15.5kD protein as sticks.

of the K-turn motif. Interestingly, all other residues outside of loop 9 participating in human 15.5kD protein−RNA interaction are well-conserved in *Giardia* 15.5kD protein.

Phylogenetic analysis of eukaryotic and archaeal 15.5kD and L7Ae proteins revealed that *Giardia* 15.5kD protein branches early in eukaryotic 15.5kD protein evolution. Its intermediate stability in both thermal and urea denaturation analysis when compared with those of *M. jannaschii* L7Ae and mouse 15.5kD protein is consistent with its early branching in 15.5kD protein evolution. The *Giardia* 15.5kD protein T_m of 63 °C is approximately 35−40 °C lower than that of *M. jannaschii* and *A. pernix* L7Ae (B. A. Brown, unpublished results) but significantly higher that the mouse 15.5kD protein T_m of 52 °C. The archaeal L7Ae proteins are typically characterized by shorter loop regions and extensive ionic interactions within their structure. Comparison of *Giardia* 15.5kD protein with human 15.5kD protein reveals shorter loop regions and an increased number of ion pair interactions, although certainly with fewer ion pairs than the *M. jannaschii* L7Ae homologue. The total number of charged residues (DEHRK) in the *Giardia* protein is 29, which is higher than the number in the human form (28) but much lower than the number in archaeal homologues of *M. jannaschii* (38) and *A. pernix* (44). In *Giardia* 15.5kD protein, a total of 15 ion pair contacts were located in chain A within the cutoff distance of 6 Å, of which four were between chains A and B (Figure 1A). The ion pair networks between chains A and B in the asymmetric unit were within 2.5−4.5 Å of each other. In comparison, 17 ion pair networks were identified in *M. jannaschii* and only five in the human 15.5kD homologue.

Despite the weak in vitro binding of *Giardia* 15.5kD protein to the K-turn motif, this core protein is able to initiate the assembly of a chimeric eukaryotic−archaeal box C/D RNP. A similar substitution of archaeal L7Ae by mouse 15.5kD protein does not assemble a box C/D complex despite its ability to bind the K-turn motif. Quite strikingly and certainly unexpectedly, the assembled chimeric complex is catalytically active and able to guide nucleotide methylation of target RNAs utilizing both the box C/D and C′/D′ RNP subcomplexes. Models for an "asymmetric" eukaryotic box C/D snoRNP structure have been built upon the observations that the 15.5kD core protein in vitro binds exclusively the K-turn motif and that the 15.5kD protein forms cross-links to the K-turn but not the K-loop.[43] Thus, this core protein was expected to be found only in the terminal box C/D RNP and not the internal C′/D′ complex. However, recent results probing archaeal box C/D sRNP structure have shown that mutation of L7Ae to disrupt K-loop binding nevertheless results in incorporation of L7Ae into the C′/D′ RNP.[17] This observation reveals the importance of core protein−protein interactions for box C/D RNP assembly, particularly the C′/D′ RNP. More recently, our work has also revealed that yeast Snu13p (15.5kD) is found in the C′/D′ RNP even though this core protein cannot bind the K-loop motif.[44] Collectively, these results reveal the importance of core protein−protein interactions for box C/D RNP assembly, particularly the C′/D′ RNP, and demonstrate that both the archaeal and eukaryotic box C/D RNPs are "symmetric" with respect to the distribution of L7Ae and 15.5kD proteins in both the terminal box C/D and internal C′/D′ RNP subcomplexes. Therefore, we expect the *Giardia* 15.5kD core protein is present in both the box C/D and C′/D′ RNPs of the chimeric complex, thus allowing each fully assembled subcomplex to guide 2′-O-methylation of their target nucleotides.

It is becoming increasingly evident that core protein−protein interactions play critical roles in box C/D RNP assembly and methyltransferase function.[13,45] Assembly of the archaeal box C/D sRNP has shown that core protein binding is sequential with L7Ae binding first followed by Nop56/58 and then fibrillarin. Binding of the L7Ae or 15.5kD protein first stabilizes the K-turn and K-loop motifs.[16] The L7Ae and 15.5kD proteins bound to the K-turn and K-loop then establish an RNP platform upon which the remaining core proteins bind utilizing not only RNA−protein interactions but also and importantly protein−protein interactions. The bound L7Ae or 15.5kD homologue presents a protein interface for interactions with the Nop and fibrillarin core proteins. Subsequent binding of Nop56/58 promotes RNA remodeling, which indicates direct interaction with the box C/D sRNA. This is consistent with the in vivo cross-linking of eukaryotic Nop56 and Nop58 to the box C/D snoRNAs.[43] Final assembly of the archaeal complex is accomplished via the addition of fibrillarin, which appears to occur primarily via protein−protein interactions with Nop56/58.[11,16] This is consistent with the very strong interaction of Nop56/58 with fibrillarin,[11] even suggesting that these two proteins may bind as a dimer during sRNP assembly. Clearly, key features of the L7Ae interface required for Nop56/58 and fibrillarin binding have been sufficiently conserved in the *Giardia* 15.5kD protein

such that the Nop56/58 and fibrillarin core proteins may bind to complete sRNP assembly. Notably, this conservation is also sufficient to allow the chimeric complex to guide nucleotide modification. Thus, the ability to assemble box C/D RNPs and guide site-specific nucleotide modification by interacting with both archaeal and eukaryotic core proteins suggests that the *Giardia* 15.5kD protein occupies a unique position in the evolution of this ancient RNA-binding protein.

Accession Codes

The coordinates and structure factors have been deposited in the Protein Data Bank as entry 3O85.

AUTHOR INFORMATION

Corresponding Author

*Department of Molecular and Structural Biochemistry, North Carolina State University, Raleigh, NC 27695. E-mail: stu_maxwell@ncsu.edu. Phone: (919) 515-5803. Fax: (919) 515-2047.

Funding Sources

This work was supported by National Institutes of Health Grant GM069699 (B.A.B.) and National Science Foundation Grant MCB 0543741 (E.S.M.).

ACKNOWLEDGMENT

We thank Dr. Paul Swartz for the availability of the in-house X-ray facilities at North Carolina State University whenever needed and members of SERCAT beamline 22ID at the Advanced Photon Source for beam time assistance.

ABBREVIATIONS

RNP, ribonucleoprotein complex; snoRNA, small nucleolar RNA; snoRNP, small nucleolar ribonucleoprotein complex; sRNA, snoRNA-like RNA; sRNP, snoRNA-like ribonucleoprotein complex; snRNP, small nuclear ribonucleoprotein complex; K-turn, kink-turn; K-loop, kink-loop; EMSA, electrophoretic mobility shift analysis; Gl, *Giardia lamblia*; Mj, *Methanocaldococcus jannaschii*; PCR, polymerase chain reaction; PDB, Protein Data Bank.

REFERENCES

(1) Decatur, W., and Fournier, M. J. (2003) RNA-guided nucleotide modification of ribosomal and other RNAs. *J. Biol. Chem. 278*, 695–698.

(2) Gagnon, K., Qu, G., and Maxwell, E. S. (2009) Multicomponent 2′-O-Ribose Methylation Machines: Evolving Box C/D RNP Structure and Function. In *DNA and RNA Modification Enzymes: Structure, Mechanism, Function and Evolution* (Grosjean, H., Ed.) pp 436−449, Landes Press, Austin, TX.

(3) Klein, D., Schmeing, T., Moore, P., and Steitz, T. (2001) The kink-turn: A new RNA secondary structure motif. *EMBO J. 20*, 4214–4221.

(4) Vidovic, I., Nottrott, S., Hartmuth, K., Lührmann, R., and Ficner, R. (2000) Crystal structure of the spliceosomal 15.5kD protein bound to a U4 snRNA fragment. *Mol. Cell 6*, 1331–1342.

(5) Nolivos, S., Carpousis, A., and Clouet-d'Orval, B. (2005) The K-loop, a general feature of the *Pyrococcus* C/D guide RNAs, is an RNA structural motif related to the K-turn. *Nucleic Acids Res. 33*, 6507–6514.

(6) Kiss-Laszlo, Z., Henry, Y., and Kiss, T. (1998) Sequence and structural elements of methylation guide snoRNAs essential for site-specific ribose methylation of pre-rRNA. *EMBO J. 17*, 797–807.

(7) Watkins, N., Ségault, V., Charpentier, B., Nottrott, S., Fabrizio, P., Bachi, A., Wilm, M., Rosbash, M., Branlant, C., and Lührmann, R. (2000) A common core RNP structure shared between the small nucleoar box C/D RNPs and the spliceosomal U4 snRNP. *Cell 103*, 457–466.

(8) Lafontaine, D., and Tollervey, D. (1999) Nop58p is a common component of the box C/D snoRNPs that is required for snoRNA stability. *RNA 5*, 455–467.

(9) Lafontaine, D., and Tollervey, D. (2000) Synthesis and assembly of the box C/D small nucleolar RNPs. *Mol. Cell. Biol. 20*, 2650–2659.

(10) Omer, A., Lowe, T., Russell, A., Ebhardt, H., Eddy, S., and Dennis, P. (2000) Homologs of small nucleolar RNAs in Archaea. *Science 288*, 517–522.

(11) Tran, E., Zhang, X., and Maxwell, E. S. (2003) Efficient RNA 2′-O-methylation requires juxtaposed and symmetrically assembled archaeal box C/D and C′/D′ RNPs. *EMBO J. 22*, 3930–3940.

(12) Omer, A., Ziesche, S., Ebhardt, H., and Dennis, P. (2002) *In vitro* reconstitution and activity of a C/D box methylation guide ribonucleoprotein complex. *Proc. Natl. Acad. Sci. U.S.A. 99*, 5289–5294.

(13) Rashid, R., Aittaleb, M., Chen, Q., Spiegel, K., Demeler, B., and Li, H. (2003) Functional requirement for symmetric assembly of archaeal box C/D small ribonucleoprotein particles. *J. Mol. Biol. 333*, 295–306.

(14) Watkins, N., Dickmanns, A., and Luhrmann, R. (2002) Conserved stem II of the box C/D motif is essential for nucleolar localization and is required, along with the 15.5K protein, for the hierarchical assembly of the box C/D snoRNP. *Mol. Cell. Biol. 22*, 8342–8352.

(15) Suryadi, J., Tran, E., Maxwell, E. S., and Brown, B. (2005) The crystal structure of the *Methanocaldococcus jannaschii* multi-functional L7Ae RNA-binding protein reveals an induced-fit interaction with the box C/D RNAs. *Biochemistry 44*, 9657–9672.

(16) Gagnon, K., Zhang, X., Agris, P., and Maxwell, E. S. (2006) Assembly of the archaeal box C/D sRNP can occur via alternative pathways and requires temperature-facilitated sRNA remodeling. *J. Mol. Biol. 362*, 1025–1042.

(17) Gagnon, K., Zhang, X., Guosheng, Q., Biswas, S., Suryadi, J., Brown, B., and Maxwell, E. S. (2010) Signature amino acids enable the archaeal L7Ae box C/D RNP core proteins to recognize and bind the K-loop motif. *RNA 16*, 79–90.

(18) Szewczak, L., DeGregorio, S., Strobel, S., and Steitz, J. (2002) Exclusive interaction of the 15.5kD protein with the terminal box C/D motif of a methylation guide snoRNP. *Chem. Biol. 9*, 1095–1107.

(19) Li, L., and Ye, K. (2006) Crystal structure of an H/ACA box ribonucleoprotein particle. *Nature 443*, 302–307.

(20) Hamma, T., and Ferre-D'Amare, A. (2004) Structure of protein L7Ae bound to a K-turn derived from an archaeal box H/ACA sRNA at 1.8 Å resolution. *Structure 12*, 893–903.

(21) Charron, C., Cléry, M. X., Senty-Ségault, V., Charpentier, B., Marmier-Gourrier, N., Branlant, C., and Aubry, A. (2004) The archaeal sRNA binding protein L7Ae has a 3D structure very similar to that of its eukaryal counterpart while having a broader RNA-binding specificity. *J. Mol. Biol. 342*, 757–773.

(22) Moore, T., Zhang, Y., Fenley, M., and Li, H. (2004) Molecular basis of box C/D RNA-protein interactions; cocrystal structure of archaeal L7Ae and a box C/D RNA. *Structure 12*, 807–818.

(23) Charron, C., Manival, X., Charpentier, B., Branlant, C., and Aubry, A. (2004) Purification, crystallization and preliminary X-ray diffraction data of L7Ae sRNP core protein from *Pyrococcus abyssii*. *Acta Crystallogr. D60*, 122–124.

(24) Lane, S., and Lloyd, D. (2002) Current trends in research into the waterborne parasite *Giardia*. *Crit. Rev. Microbiol. 28*, 123–147.

(25) Bleichert, F., Gagnon, K. T., Brown, B., Maxwell, E. S., Leschziner, A. E., Unger, V. M., and Baserga, S. (2009) A dimeric structure for archaeal box C/D small ribonucleoproteins. *Science 325*, 1384–1387.

(26) Otwinowsky, Z., and Minor, W. (1997) Processing of X-ray diffraction data collected in oscillation mode. *Methods Enzymol. 276*, 307–326.

(27) Oruganti, S., Zhang, Y., and Li, H. (2005) Structural comparison of yeast snoRNP and spliceosomal protein Snu13p with its homologs. *Biochem. Biophys. Res. Commun. 333*, 550–554.

(28) McCoy, A., Grosse-Kunstleve, R., Adams, P., Winn, M., Storoni, L., and Read, R. (2007) Phaser crystallographic software. *J. Appl. Crystallogr. 40*, 658–674.

(29) Emsley, P., and Cowtan, K. (2004) Coot: Model-building tools for molecular graphics. *Acta Crystallogr. 60*, 2126–2132.

(30) Brunger, A., Adams, P., Clore, G., Delano, W. L., Gros, P., Grosse-Kunstleve, R., Jiang, J., Kuszewski, J., Nilges, M., Pannu, N., Read, R., Rice, L., Simonson, T., and Warren, G. (1998) Crystallography and NMR system: A new software suite for macromolecular structure determination. *Acta Crystallogr. D54*, 905–921.

(31) Adams, P., Afonine, P., Bunkóczi, G., Chen, V., Davis, I., Echols, N., Head, J., Hung, L., Kapral, G., Grosse-Kunstleve, R., McCoy, A., Moriarty, N., Oeffner, R., Read, R., Richardson, D., Richardson, J., Terwilliger, T., and Zwart, P. (2010) PHENIX: A comprehensive Python-based system for macromolecular structure solution. *Acta Crystallogr. D66*, 213–221.

(32) Laskowski, R., MacArthur, M., Moss, D., and Thornton, J. (1993) PROCHECK: A program to check the stereochemical quality of protein structures. *J. Appl. Crystallogr. 26*, 283–291.

(33) Davis, I., Leaver-Fay, A., Chen, V., Block, J., Kapral, G., Wang, X., Murray, L., Arendall, W., Snoeyink, J., Richardson, J., and Richardson, D. (2007) MolProbity: All-atom contacts and structure validation for proteins and nucleic acids. *Nucleic Acids Res. 35*, W375–W383.

(34) Kleywegt, G. (1999) Experimental assessment differences between related protein crystal structures. *Acta Crystallogr. D55*, 1878–1857.

(35) DeLano, W. (2002) *The PyMOL Molecular Graphics System*, DeLano Scientific, San Carlos, CA.

(36) Larkin, M., Blackshields, G., Brown, N., Chenna, R., McGettigan, P., McWilliam, H., Valentin, F., Wallace, I., Wilm, A., Lopez, R., Thompson, J., Gibson, T., and Higgins, D. (2007) ClustalW and ClustalX version 2. *Bioinformatics 23*, 2947–2948.

(37) Tamura, K., Dudley, J., Nei, M., and Kumar, S. (2007) MEGA4: Molecular Evolutionary Genetics Analysis (MEGA) software version 4.0. *Mol. Biol. Evol. 24*, 1596–1599.

(38) Marky, L., and Breslauer, K. (1987) Calculating thermodynamic data for transitions of any molecularity from equilibrium melting curves. *Biopolymers 26*, 1601–1620.

(39) Chao, J., Prasad, G., White, S., Stout, D., and Williamson, J. (2003) Inherent protein structural flexibility at the RNA-binding interface of L30e. *J. Mol. Biol. 326*, 999–1004.

(40) Dlakić, M. (2005) 3D models of yeast RNase P/MRP proteins Rpp1p and Pop3p. *RNA 11*, 123–127.

(41) Donovan, J., and Copeland, P. (2009) Evolutionary history of selenocysteine incorporation from the perspective of SECIS binding proteins. *BMC Evol. Biol. 9*, 1–18.

(42) Khanna, M., Wu, H., Johansson, C., Caizergues-Ferrer, M., and Feigon, J. (2006) Structural study of the H/ACA snoRNP components Nop10p and the 3′ hairpin of U65 snoRNA. *RNA 12*, 40–52.

(43) Cahill, N., Friend, K., Speckmann, W., Li, Z., Terns, R., Terns, M., and Steitz, J. (2002) Site-specific cross-linking analyses reveal an asymmetric distribution for a box C/D snoRNP. *EMBO J. 21*, 3816–3828.

(44) Qu, G., van Nues, R., Watkins, N., and Maxwell, E. S. (2011) The spatial-functional coupling of the box C/D and C′/D′ RNPs is an evolutionarily conserved feature of the eukaryotic box C/D snoRNP nucleotide modification complex. *Mol. Cell. Biol. 31*, 365–374.

(45) Zhang, X., Champion, E., Tran, E., Brown, B., Baserga, S., and Maxwell, E. S. (2006) The coiled-coil domain of the Nop56/58 core protein is dispensable for sRNP assembly but is critical for archaeal box C/D sRNP-guided nucleotide methylation. *RNA 12*, 1092–1103.